Photochemical & Photobiological Sciences

Cite this: DOI: 10.1039/c2pp25210d

www.rsc.org/pps

PAPER

Photochemistry of 1-allyl-4-aryltetrazolones in solution; structural effects on photoproduct selectivity†

Amin Ismael,[a] Carlos Serpa[b] and M. Lurdes S. Cristiano*[a]

Received 21st June 2012, Accepted 24th August 2012
DOI: 10.1039/c2pp25210d

The photochemistry of tetrazolones derived from the carbocyclic allylic alcohols cyclohex-2-enol and 3-methylcyclohex-2-enol and from the natural terpene alcohol nerol was investigated in solution with the aim of assessing the effect of solvent and of structural constraints imposed by bulky allylic moieties on photoproduct selectivity and stability. Photolysis of tetrazolones derived from nerol and cyclohex-2-enol afforded the corresponding pyrimidinones as major products through a pathway that appears to be similar to that proposed for other 1-allyl-4-phenyl-1,4-dihydro-5*H*-tetrazol-5-ones derived from acyclic and unhindered allylic alcohols previously investigated but photolysis of the tetrazolone derived from the bulkier 3–methylcyclohex-2-enol **4c** leads to formation of a benzimidazolone, indicating that, in this case, cyclization of the biradical formed upon extrusion of N_2 involves the phenyl substituent and not the allylic moiety. Theoretical calculations (DFT(B3LYP)/3-21G*) were conducted to support the interpretation of the experimental results and mechanistic proposals. Laser flash photolysis experiments were conducted with the aim of clarifying the nature of the intermediate involved in the primary photocleavage process.

1. Introduction

Tetrazole[1] and its derivatives are applied in major areas, such as medicine, agriculture, food chemistry and imaging technology. Most applications of tetrazoles derive from the acid/base properties of the tetrazolic acid fragment, $–CN_4H$, which acts as a surrogate for the carboxylic acid group, $–CO_2H$, due to its comparatively higher metabolic stability at physiological pH.[2]

The photochemistry of tetrazole and a range of its derivatives has been studied, in solution and/or isolated in cryogenic matrices.[3–27] Photodecomposition of tetrazoles involves cleavage of the tetrazolyl ring, leading to a variety of photoproducts. Azides, isocyanates or aziridines are generally obtained, but the presence of labile hydrogen atoms, either directly linked to the tetrazole ring or in substituent groups, may open additional photocleavage pathways or allow for secondary photochemical reactions to take place concomitantly with the main primary photoprocesses.[4–8,20–26] The photochemistry of tetrazoles is also influenced by the chemical nature and conformational flexibility of substituents linked to the heterocycle, which may favor or exclude certain reaction channels,[9–14] determining the nature and relative amount of the final photoproducts.

The photochemistry of tetrazoles in solution has been reviewed in the context of potential applications to organic synthesis.[28] Analysis of the literature reveals that, through a careful selection of the solvent and other reaction conditions, the photofragmentation of some derivatives of tetrazole may be tuned to grant selectivity and high yield, affording stable and synthetically useful photoproducts that may be isolated and stored, or trapped in the reaction media. A diversity of photoproducts such as 9*H*-pyrimido(4,5-*b*)indoles,[24] diaziridinones,[16,25] iminoaziridines,[26,27] carbodiimides,[22,25] oxazines,[14] benzimidazolones[22] and pyrimidinones[10,11] may be obtained from photolysis of tetrazole derivatives in solution. Of the 7 classes mentioned, 3 (diaziridinones, benzimidazolones and pyrimidinones) result from photolysis of 1,4-disubstituted-1,4-dihydro-5*H*-tetrazol-5-ones (tetrazolones), illustrating their versatility as starting materials for the preparation of other scaffolds and the relevance of a deep investigation of the photochemistry of this particular class.

The synthesis of benzimidazolones from photolysis of 4-substituted-1,4-dihydro-1-phenyl-5*H*-tetrazol-5-ones was reported in 1985.[22] The authors described that irradiation of 1-phenyl-tetrazolones substituted at *N*-4 by hydrogen, phenyl, alkyl, propenyl and butenyl, in methanol, acetonitrile or 2-propanol leads to benzimidazolones as final products in nearly quantitative yields and proposed a mechanism involving photoextrusion of molecular nitrogen with formation of a biradical intermediate that, upon cyclization involving the phenyl substituent, gives rise to the product.[22]

The photochemistry in solution of a small range of 1-allyl-4-phenyl-1,4-dihydro-5*H*-tetrazol-5-ones was investigated in our group.[10,11] Tetrazolones **4** (Scheme 1; R = H, CH_3, Ph) were

[a]*CCMAR and Department of Chemistry and Pharmacy, F.C.T., University of Algarve, P-8005-039 Faro, Portugal. E-mail: mcristi@ualg.pt*
[b]*Department of Chemistry, University of Coimbra, P-3004-535 Coimbra, Portugal*

†Electronic supplementary information (ESI) available. See DOI: 10.1039/c2pp25210d

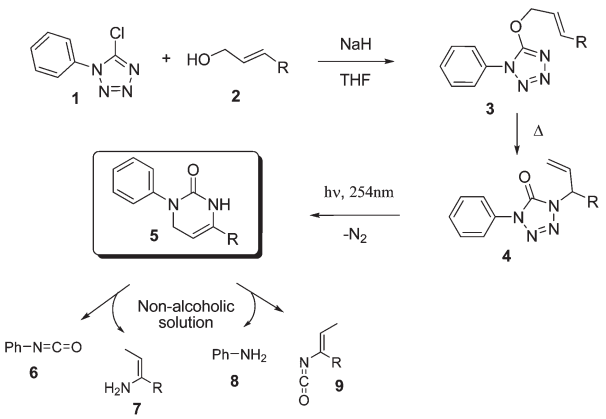

Scheme 1 Proposed synthetic route to pyrimidinones from allylic alcohols, based on photolysis of tetrazolones in alcohols.

irradiated in cyclohexane, acetonitrile, methanol, 1-propanol and 1-hexanol. Photolysis of the compounds in all solvents tested resulted in formation of 3,4-dihydro-6-substituted-3-phenylpyrimidin-2(1*H*)-ones **5** as the sole primary photoproducts. Based on the observed photosensitizing effect of oxygen and on the observation that an increase in solvent viscosity leads to a decrease in quantum yields we proposed that photoexcitation of 1-allyl-4-phenyl-1,4-dihydro-5*H*-tetrazol-5-ones **4** would lead to photoextrusion of molecular nitrogen with possible formation of a caged triplet biradical that after T–S conversion would cyclize to form pyrimidinones **5** that, in the protic solvents, remained photostable even after extended periods of irradiation.[11] Besides, formation of a biradical from tetrazolones, through photolysis, had already been postulated.[22] When irradiation was conducted in cyclohexane, carbon tetrachloride or acetonitrile, the primary photoproducts **5** underwent rapid photodecomposition to afford a mixture of products identified as allyl amine **7**, aniline 8 phenyl-, and allyl-isocyanates (**6**, **9**, Scheme 1).

Given the observed selectivity and stability of compounds **5** in alcohols, we postulated that the novel synthetic route to pyrimidinones from allylic alcohols in only 3 steps (Scheme 1) should be further explored. Besides, 5-allyloxy-1-aryl tetrazoles **3** are prepared in high yields from the reaction of the required allylic alcohol **2** with 5-chloro-1-phenyl tetrazole **1**[29] and 1-allyl-4-aryl-tetrazolones **4** are obtained from 5-allyloxy-1-aryl tetrazoles **3**, in quantitative yields, through a thermally-induced sigmatropic isomerisation that proceeds *via* a concerted [3,3′]-sigmatropic Claisen-type mechanism.[30–33]

Considering the relevance of pyrimidinones as scaffolds in heterocyclic synthesis[34] and the importance of developing mild and efficient synthetic routes to these compounds, we aimed at a deeper investigation of the scope of this photochemically based synthetic methodology. In particular, we propose to study the effect of steric constraints imposed by bulky allylic moieties on photoproduct selectivity and stability. In this publication, we describe the photochemistry of tetrazolones derived from the natural terpene nerol **4a** (see Scheme 2) and from the cyclic allyl alcohols cyclohex-2-enol **4b** and 3-methylcyclohex-2-enol **4c** (Scheme 3). Tetrazolones **4a–c** were prepared and subsequently irradiated in methanol, acetonitrile and cyclohexene. Results show that photolysis of tetrazolones **4a,b** leads to formation of

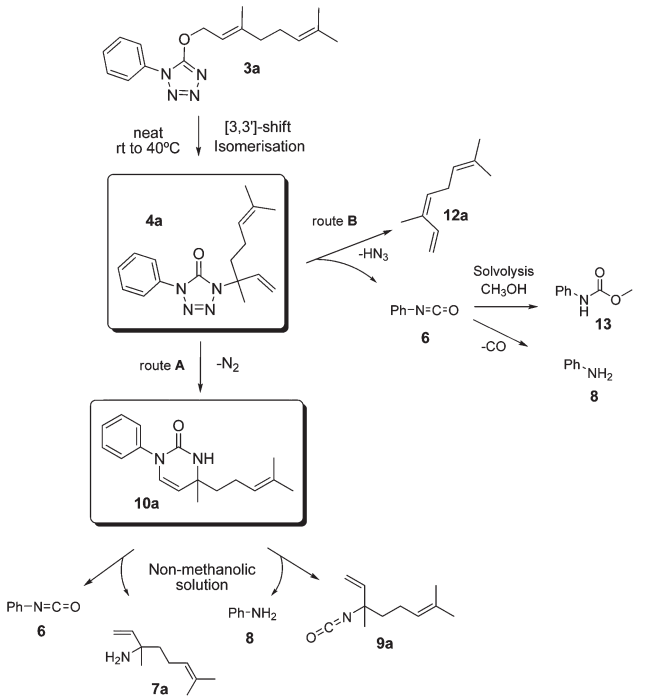

Scheme 2 Proposed photodegradation pathways of 1-(3,7-dimethyl-octa-1,6-dien-3-yl)-4-phenyl-1*H*-tetrazol-5(4*H*)-one **4a** in solution.

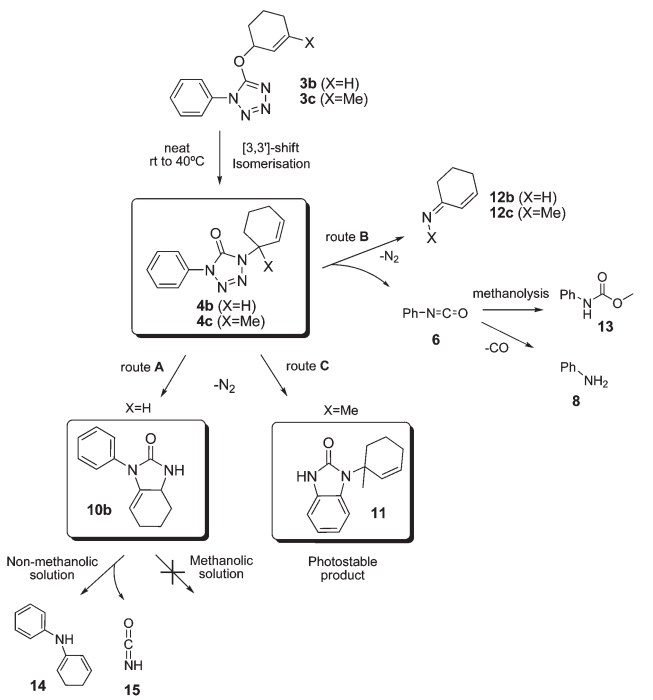

Scheme 3 Proposed photodegradation pathways of 1-cyclohexenyl-4-phenyl tetrazolones **4b,c** in solution.

compounds **10a,b** through a pathway that appears to be similar to that proposed for other 1-allyl-4-phenyl-1,4-dihydro-5*H*-tetrazol-5-ones previously investigated,[10,11] but photolysis of the tetrazolone derived from the bulkier 3-methylcyclohex-2-enol **4c** leads to formation of benzimidazolone **11**, indicating that, in this

case, cyclization of the transient intermediate species formed upon extrusion of N_2 involves the phenyl substituent and not the allylic moiety. This unexpected cyclization pathway is ascribed to steric constraints imposed by the methyl group attached to the allylic carbon in **4c**, which hinders the cyclization pathway involving the intermediate formed from **4c** and the allylic system, that would lead to formation of the expected pyrimidinone. Interpretation of the experimental results was assisted by theoretical calculations (DFT(B3LYP)/3-21G*). Laser flash photolysis experiments were conducted with the aim of clarifying the nature of the transient intermediate species involved in the primary photocleavage.

2. Results and discussion

2.1. Synthesis of tetrazolones 4a–c

Synthesis of 1-allyl-4-phenyltetrazolones **4a–c** (Schemes 2 and 3) was conducted following the methodology depicted in Scheme 1. The carbocyclic allylic alcohols cyclohex-2-enol and 3-methylcyclohex-2-enol and nerol were converted into the allylic alkoxides through reaction with sodium hydride in anhydrous conditions. Subsequent addition of 5-chloro-1-phenyltetrazole[29] resulted in nucleophilic displacement of chloride leading to formation of 5-allyloxy-1-phenyltetrazoles **3a–c**. Ethers **3a,b** could be isolated and characterised. However, putative ether **3c** could not be isolated, as it readily isomerised to the corresponding tetrazolone **4c**, under the conditions used for etherification. It was also observed that isomerization of ether **3a** occurs very easily at room temperature. *N*-Allyl-tetrazolones **4a,b** were quantitatively obtained from the corresponding ethers **3a,b** by heating a neat sample. ^{1}H-NMR spectra for compounds **4a–c** are presented in Fig. S1–S3 (ESI†).

2.2. Photolysis of 1-allyl-4-phenyltetrazolones 4a–c

Solutions of *N*-allyl-tetrazolones **4a–c** in methanol, acetonitrile and cyclohexane were irradiated with a low-pressure mercury lamp (λ = 254 nm) and the reaction was monitored by GC-MS. Irradiation was continued until no starting material was detected. GC-MS analysis of irradiated solutions led to the identification of one major primary photoproduct for each of the three derivatives. Preparative-scale irradiations were conducted, followed by purification of the photoproducts by column chromatography on silica gel. Analysis of the isolated products by mass spectrometry (EI) and ^{1}H-NMR (see Fig. S4–S6; ESI†) confirmed their structures. No degradation of the photoproducts during storage was observed.

Fig. S7 (ESI†) shows the UV spectra of methanolic solutions of tetrazolones **4a–c** (blue) and of photoproducts **10a,b** and **11** (red). As shown, the UV spectral assignments for compounds **4a–c** are similar, with absorption maxima around 249 nm, indicating that, for these 3 compounds, the structure of the *N*-allyl substituents attached to the tetrazolyl ring has a negligible effect on the absorbance of the chromophore. UV spectra for compounds **10a,b** exhibit similar patterns, with maxima of 241 and 238 nm respectively, and are also similar to spectra of pyrimidinones previously obtained from photolysis of other 1-allyl-4-phenyltetrazolones.[10,11] Note that the photoproduct **10a** shows absorbance at the excitation wavelength and thus photolysis yields will decrease at higher conversions, which may explain why photolysis of tetrazolone **4a** is comparatively slower. Photoproduct **10b** also shows absorbance at the excitation wavelength, and photolysis yield would also be expected to decrease at higher conversions. However, it was observed that photofragmentation through route B (Scheme 3) is higher, resulting in an overall faster photodegradation of tetrazolone **4b** when compared to **4a** (see Fig. S9, ESI†).

As observed, the UV spectrum of compound **11**, resulting from photolysis of **4c**, shows a different pattern from those exhibited by photoproducts **10a** and **10b**. As discussed below, the intermediate species formed from photolysis of **4c** follows an alternative cyclisation pathway, leading to a benzimidazolone.

The molar absorption coefficients (ε) for tetrazolones **4a–c** and photoproducts **10a,b** and **11**, calculated at λ_{max}, are provided in Table S11.† A detailed description of the results obtained for steady-state photolysis of compounds **4a–c** is provided below.

2.2.1. Photolysis of 1-(3,7-dimethylocta-1,6-dien-3-yl)-4-phenyl-1*H*-tetrazol-5(4*H*)-one (4a). Photolysis of tetrazolone **4a** was initially conducted in methanol. The major photoproduct, identified as 4-methyl-4-(4-methylpent-3-enyl)-1-phenyl-3,4-dihydropyrimidin-2(1*H*)-one **10a** (Scheme 2), was isolated in 83% yield after purification by column chromatography on silica gel. This primary photoproduct is formed by extrusion of molecular nitrogen from the tetrazolyl ring system in **4a** through photo-induced cleavage of the two formally single N–N bonds of the heterocycle followed by cyclization of the resulting transient intermediate involving the allylic fragment (route A; Scheme 2). GC-MS analysis of this primary photoproduct shows a peak with a shoulder that we assumed to result from the presence of a mixture of conformers, which was supported by analysis of the ^{1}H NMR spectrum where two sets of signals with small differences in chemical shifts are observed (see Fig. S4 and S8; ESI†).

Traces of other primary photoproducts were identified: phenyl-isocyanate (**6**; *m*/*z* = 119), that is subsequently converted to *N*-phenyl methylcarbamate (**13**; *m*/*z* = 151), through methanolysis, or aniline (**8**; *m*/*z* = 93), through hydrolysis followed by decarboxylation, and a peak that matches the MS trace of 3,7-dimethyl-1,3,6-octatriene (**12a**; *m*/*z* = 136) resulting from 3-azido-3,7-dimethyl-1,6-octadiene through elimination of azide. Phenyl isocyanate, aniline and *N*-phenyl methylcarbamate were identified by comparing their GC-MS spectra with those of standard samples of the compounds. The identification of these minor photoproducts on the GC/MS spectra from the beginning of irradiation clearly indicates that two photo-fragmentation pathways (A and B; Scheme 2) for tetrazolone **4a** are at play. In order to confirm that compounds **6**, **8**, **12a** and **13** were generated from an alternative photocleavage of **4a** and not by photocleavage of the major primary photoproduct resulting from pathway A, a pure sample of compound **10a** was irradiated in methanol, using the experimental conditions applied to photolysis of **4a**. Even with extended irradiation, no secondary photoproducts were detected, confirming that compounds **6**, **8**, **12a**, **13** result from tetrazolone photodegradation and demonstrating that pyrimidinone **10a** is photostable in methanol. Thus, a minor photofragmentation route B, involving photocleavage of the

formally single N–N and C–N bonds on tetrazolone **4a** and leading to trace amounts of phenyl-isocyanate and 3-azido-3,7-dimethyl-1,6-octadiene, operates concomitantly with the major photofragmentation/cyclisation pathway A.

Based on previous work,[35] we expected to observe extrusion of molecular nitrogen from the putative primary photoproduct 3-azido-3,7-dimethyl-1,6-octadiene, followed by rearrangement, leading to the corresponding imine derivative. As will be described below, this was observed for tetrazolones **4b** and **4c**. However, with tetrazolone **4a** no imine was ever detected. We believe that the preferential elimination of azide from 3-azido-3,7-dimethyl-1,6-octadiene results from the high stability of the conjugated diene system formed in the **12a** photoproduct.

The photoreactivity of *N*-allyl-tetrazolone in acetonitrile and cyclohexane was also investigated and proved to be similar to that in methanol. Photolysis of **4a** may occur through pathway A, leading to compound **10a** as the major primary photoproduct, and through pathway B, leading to phenyl-isocyanate and subsequently to aniline. The relative concentrations of phenyl-isocyanate and aniline are higher than those obtained when photolysis was conducted in methanol. It has been reported that pyrimidinones undergo easy photocleavage in non-alcoholic solvents.[10,11] Thus, the higher formation of phenyl-isocyanate and aniline can be explained by ring photocleavage of pyrimidinone **10a** (Scheme 2). This was confirmed by irradiating solutions of pyrimidinone **10a**, isolated previously as the major product of photolysis in methanol, in acetonitrile and cyclohexane. These experiments led to formation of phenyl-isocyanate and aniline, confirming that the two products also result from pyrimidinone photodegradation. The formation of phenyl-isocyanate and aniline by photocleavage of **10a** will be concomitant with formation of two other possible secondary products (**7a**, **9a**, respectively). However, these photoproducts were never detected, due possibly to their high volatility, fast photodecomposition into low molecular weight products, or fast elution under the chromatographic conditions used.

2.2.2. Photolysis of 4-(cyclohex-2-enyl)-1-phenyl-1*H*-tetrazol-5(4*H*)-one (4b). Photolysis in 4-(cyclohex-2-enyl)-1-phenyl-1*H*-tetrazole-5-one **4b** in methanol using the experimental conditions applied with **4a** led to formation of a main primary photoproduct, isolated in 56% yield and identified as 1-phenyl-3a,4,5,6-tetrahydro-1*H*-benzoimidazol-2(3*H*)-one **10b** (Scheme 3). This compound results from route A, a pathway that involves photoextrusion of molecular nitrogen from the tetrazolyl ring followed by cyclization of the resulting transient intermediate involving the allylic moiety. In order to distinguish the photoproducts resulting from different cyclization pathways, with the allylic moiety or the phenyl ring, we shall class photoproduct **10b** as a pyrimidinone.

As observed for photolysis of **4a**, a second photocleavage pathway (route B) leading to phenyl-isocyanate (**6** m/z = 119) and corresponding products of solvolysis *N*-phenyl methylcarbamate (**13** m/z = 151) and aniline (**8** m/z = 93), together with cyclohex-2-enimine (**12b** m/z = 95), was also observed for compound **4b** (Scheme 3). As previously reported,[35] cyclohex-2-enimine is formed from 3-azido-cyclohexene *via* elimination of nitrogen followed by rearrangement.

Photolysis of tetrazolone **4b** in acetonitrile and cyclohexane led to formation of a new photoproduct identified as *N*-1,3-cyclohexadienyl-*N*-phenylamine **14**, arising from photocleavage of primary photoproduct **10b** (Scheme 3). Proposal of this pathway was confirmed through irradiation experiments using a pure sample of pyrimidinone **10b** (isolated previously from photolysis in methanol) in acetonitrile and cyclohexane. In the course of these experiments, formation of this new photoproduct was detected, confirming that it results from photodegradation of the primary photoproduct **10b**.

In general terms, the outcome of photolysis in compounds **4a** and **4b** appears to be similar, despite the cyclic nature of the allylic moiety in **4b**. The difference is the relative extent of photocleavage through route B, which represents around 40% in **4b** against less than 10% in **4a**, as shown from kinetics (discussed below).

2.2.3. Photolysis of 4-(3-methylcyclohex-2-enyl)-1-phenyl-1*H*-tetrazol-5(4*H*)-one (4c). Photolysis of 4-(3-methylcyclohex-2-enyl)-1-phenyl-1*H*-tetrazol-5(4*H*)-one **4c** in methanol resulted in a main photoproduct isolated in 76% yield and identified as 3-(1-methylcyclohex-2-enyl)-benzoimidazol-2(1*H*)-one **11**. As observed for the other allyltetrazolones studied, the primary photofragmentation route for compound **4c** involves photoextrusion of molecular nitrogen from the tetrazolyl ring system, leading to a transient intermediate species. However, a distinct process of cyclization of the intermediate appears to take place in this case (route C), leading to formation of benzimidazolone **11** (Scheme 3). Thus, the intermediate does not cyclise using the allyl moiety but, instead, uses the phenyl ring system.

Results obtained for photolysis of tetrazolone **4c** in acetonitrile and cyclohexane were similar to those obtained in methanol. Irradiation experiments using a pure sample of benzimidazolone **11** (isolated previously from photolysis in methanolic solution) in acetonitrile and cyclohexane showed that benzimidazolone **11** is a photostable product in all solvents tested.

A previous investigation on the UV-induced photochemistry ($\lambda \geq 235$ nm) of 1-phenyl-4-allyl-tetrazolone isolated in solid argon showed a photofragmentation pathway involving a [3 + 2] pericyclic molecular nitrogen elimination reaction, leading to 1-allyl-2-phenylaziridinone that subsequently forms the corresponding benzimidazolone.[12] Thus, in the cryogenic matrix, cyclization with phenyl appears more favorable than with allyl. However, when photolysed in solution, this and two other 4-allyl-tetrazolones investigated afforded pyrimidinones as the sole primary photoproducts in almost quantitative yields, and no trace of benzimidazolone was ever detected.[10,11] This trend is followed by tetrazolones **4a** and **4b**, as explained above, but not by tetrazolone **4c**. A search in the literature revealed similarities between the UV spectrum of compound **11** (Fig. S7†) and typical UV spectra of benzimidazolones,[36] adding further evidence to the identification of the photoproduct resulting from photolysis of tetrazolone **4c** as benzimidazolone **11**.

In order to shed some light on the effect of structural constraints in the allylic system on the mechanism of cyclization, and product selectivity, molecular orbital calculations at the DFT level of theory were carried out. Tetrazolones **4b** and **4c** have high structural similarity, differing only in a methyl group strategically attached to the allylic carbon. For pyrimidinone

formation, the allylic system is involved in ring closure of the transient intermediate formed from photo-extrusion of nitrogen, and this cyclisation requires prior rotation of the allylic fragment on the putative biradical. In the case of **4c** the bulky methyl group attached to the allylic carbon appears to hinder rotation of the allylic system, preventing ring closure to the expected pyrimidinone. Instead, cyclization involving the phenyl ring is preferred, leading to the observed photoproduct **11**. Results obtained from DFT calculations will be discussed in detail.

2.3. Kinetics for the photodecomposition of tetrazolones 4a–c

Fig. S9† shows the kinetics for the photodecomposition of tetrazolones **4a–c** in methanol, along with the kinetics of photoproducts formation. After 10 min of irradiation, about 90% of the tetrazolones **4a–c** had been consumed. Complete photodecomposition of tetrazolones **4b** and **4c** occurs after 15 and 20 min, respectively, but for tetrazolone **4b** formation of photoproducts through route B is more significant. After total conversion, 40% of photoproducts derived from route B were formed from tetrazolone **4b**, against 15% from tetrazolone **4c**. For tetrazolone **4a** complete photodecomposition was comparatively slower, probably due to its absorbance wavelength, as previously discussed. After 40 min of irradiation the reagent was totally consumed, and photoproducts arising from route B corresponded to less than 10%.

Fig. S10† shows the kinetic profiles for the photodecomposition of tetrazolones **4a–c** in acetonitrile, along with those for photoproducts formation. It can be deduced that photolysis in acetonitrile follows the global pattern observed in methanol, with two significant changes: the first corresponds to a significant increase in the amount of isocyanate and aniline that results from photolysis of **4a**, in keeping with previous observations showing that these photoproducts also result from photodegradation of the primary photoproduct **10a**. Also, as discussed above, photolysis of tetrazolone **4b** in acetonitrile led to formation of a new secondary photoproduct (**14**, Scheme 3), identified in Fig. S10† as an amine.

Kinetics for the photodecomposition of tetrazolones **4a–c** in cyclohexane exhibits a similar profile to that observed in acetonitrile.

2.4. Theoretical analysis of proposed routes; interpretation of substituent effects on route selectivity

The major primary photoproducts arising from photolysis of **4b** and **4c**, pyrimidinone **10b** and benzimidazolone **11**, respectively, result from elimination of nitrogen from the tetrazole ring followed by two distinct processes of cyclization. Differences in photoreactivity for the two tetrazolones can be ascribed to substitution at the allylic carbon; replacement of hydrogen by methyl clearly affects the reactivity and stability of the intermediate species involved.

In order to gather more information regarding the mechanisms involved in each case and on the specific nature of substituent effects on route selectivity, quantum chemical calculations were performed at the DFT level of theory for compounds **4b** and **4c**, considering all steps from starting tetrazolone to observed

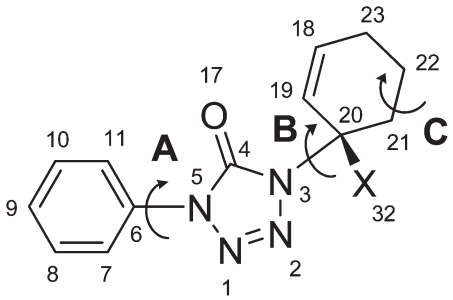

Fig. 1 Structure of the tetrazolones **4b** (X = H) and **4c** (X = CH_3) with chosen atom numbering. Carbon atom C(20) of the cyclohex-2-enyl ring is chiral. Arrows accompanied by the letters A, B and C show intramolecular conformationally revelant degrees of freedom.

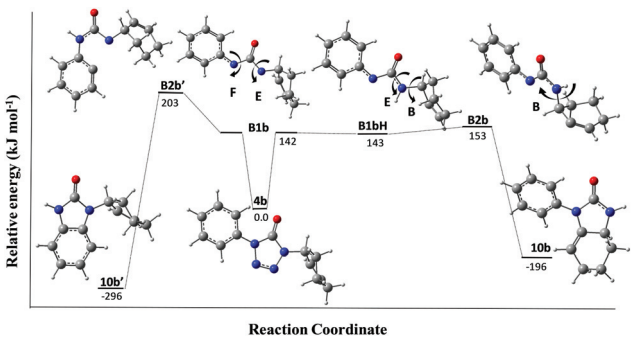

Fig. 2 Relative energies of the structures corresponding to the most stable stationary points for the photochemical formation of pyrimidinone **10b** and putative benzoimidazolone **10b′** from tetrazolone **4b**, calculated at the DFT(B3LYP)/3-21G* level.

products, pyrimidinone and benzimidazolone. Two possibilities were explored for cyclization of the transient intermediates: rotation and ring closure involving either the allylic system or the phenyl ring. Results are schematically presented in Fig. 2 and 5.

The starting compounds, 4-allyl tetrazolones **4b** and **4c**, have three intramolecular rotational degrees of freedom (designated in Fig. 1 by arrows) that may result in different conformers. These include: (i) relative orientation of the phenyl and tetrazolyl rings (dihedral angle A); (ii) relative orientation of the cyclohex-2-enol and tetrazole rings (dihedral angle B). It is important to note that the carbon atom C(20) is chiral. In the present study all calculations were carried out for the *S*-enantiomer of the starting compound; (iii) conformation of the cyclohex-2-enol ring (dihedral angle C).

Extensive chemical calculations for initial structures **4b** and **4c** were previously reported by our group.[33] Calculations at DFT level predict that in all conformers the phenyl and tetrazole rings have planar geometries and are coplanar to each other (dihedral angle A). The exchange of the substituent X (H or CH_3) does not influence this parameter. The calculated values of the dihedral angle C were found to fall in a narrow range, which indicates the rigidity of the cyclohex-2-enol ring. Dihedral angle B has the most flexible conformational degree. For tetrazolone **4b** two minima were found, corresponding to the *cis* and *trans* orientations of the CNCH (dihedral angle B), the *cis* conformer

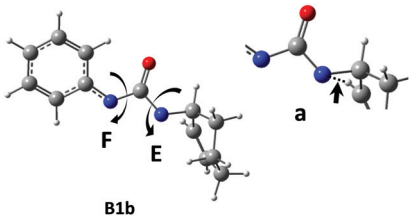

Fig. 3 Structure of the biradicalar intermediate **B1b** calculated at the DFT(B3LYP)/3-21G* level. The two new rotational degrees of freedom involve dihedrals E [OCN(3)C(20)] and F [OCN(5)C(6)] (see Fig. 1 for atom numbering). Model structure **a** illustrates the relative proximity of the nitrogen radical and the H-allylic system when rotation about E is in *cis* orientation.

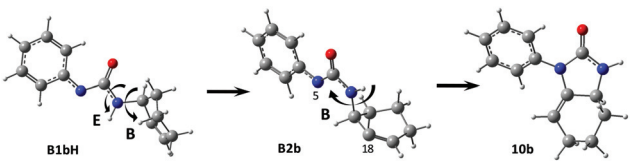

Fig. 4 Structures corresponding to minima for biradical intermediates **B1bH** and **B2b**, resulting from rotation of dihedral E, corresponding to *cis* and *trans* orientations, respectively. Considering that C(18) approaches N(5) in **B2b** through rotation of dihedral B with formation of a new C–N single bond leads to **10b**, the structure of pyrimidinone experimentally obtained.

being the most stable. The methylated tetrazolone **4c** exhibits three minima for the rotation of the CNC(20)C(21) (dihedral angle B), the *trans* and *gauche* orientations, the *gauche* (+61.4°) conformer being the most stable.

In calculations undertaken for both routes, the relative zero level of energy was chosen to be the energy of the most stable conformer of starting tetrazolones. The proposed reaction pathways and relative energies of species involved, for formation of pyrimidinone **10b** and benzimidazolone **11**, from **4b** and **4c** respectively, are presented in Fig. 2 and 5.

2.4.1. Theoretical investigation of the photodegradation of 4-(cyclohex-2-enyl)-1-phenyl-1*H*-tetrazol-5(4*H*)-one (4b). The mechanism of photocleavage of compound **4b** was investigated. Calculations were performed for the 2 putative routes. For each pathway, structures of the species proposed/observed were optimized. Fig. 2 presents a diagram of the relative energies of species corresponding to the most stable stationary points for both pathways.

Based on the literature,[11,22] we postulated that cleavage of the tetrazole ring with N_2 extrusion leads to a biradicalar intermediate **B1b** (see Fig. 3). This intermediate has two new rotational degrees of freedom, the OCN(3)C(20) (dihedral angle E) and the OCN(5)C(6) (dihedral angle F).

Two minima were found for rotation of dihedral E, corresponding to *cis* and *trans* orientations. In the *cis* orientation, the relative proximity of the nitrogen radical and the H-allylic system is noteworthy (see structure **a**). Under such circumstances, the H-migration involving the allylic system can be easily established (see structure **B1bH**, Fig. 4). We can assume that the expected H-migration is intramolecular, since it occurred

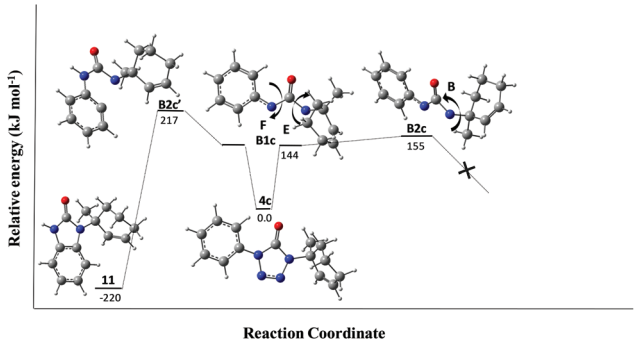

Fig. 5 Relative energies of structures corresponding to the most stable stationary points in the pathway leading to formation of benzoimidazolone **11** from tetrazolone **4c**, calculated at the DFT(B3LYP)/3-21G* level.

in the aprotic solvents acetonitrile and cyclohexane as well as in protic methanol.

From internal rotation about the B dihedral angle, when dihedral E is in the *cis* orientation (structure **B1bH**) conformations where the cyclohex-2-enol ring is directed to the carbonyl group of the tetrazole moiety can be expected, although corresponding to high energy structures due to steric hindrance. The relevant low energy forms result from this B internal rotation in the *trans* orientation of the dihedral E (see structure **B2b**), since only in this case the allylic fragment is properly aligned for ring closure. For the minima found, **B2b**, with two possible directions of internal rotation of dihedral B, a clockwise rotation of the cyclohex-2-enol moiety is essential for ring closure, due to higher steric hindrance through the counterclockwise rotation when the cyclohex-2-enol ring is directed to the phenyl group. Subsequent reaction coordinate calculations, considering that C(18) approaches N(5) through rotation of dihedral B and formation of a new C–N single bond, provided the expected structure of pyrimidinone **10b**, in an exothermic process (see Fig. 2 and 4).

The possibility of rotation and ring closure involving the phenyl ring was also studied, although the putative photoproduct (**10b′**) was never detected experimentally. For this alternative route involving rotation of dihedral angle F (Fig. 2 and 3), two minima were found, corresponding to the *cis* and *trans* orientations (**B2b′**). Calculations show that this pathway is energetically more demanding as compared with the former one. The energy calculated for intermediate (**B2b′**) is 60 kJ mol^{-1} and 50 kJ mol^{-1} higher than that for intermediates **B1bH** and **B2b**, respectively. Thus, although putative benzimidazolone **10b′** is calculated to be thermochemically more stable than pyrimidinone **10b** by around 100 kJ mol^{-1}, only the pyrimidinone is formed, through kinetic control.

2.4.2. Theoretical analysis of the photodegradation of 4-(3-methylcyclohex-2-enyl)-1-phenyl-1*H*-tetrazol-5(4*H*)-one (4c). The mechanism of photolysis of compound **4c** was investigated. As above, calculations were performed for the 2 putative routes and all structures for species proposed/observed were optimized. Fig. 5 presents a diagram of the relative energies calculated for species corresponding to the most stable stationary points for both pathways.

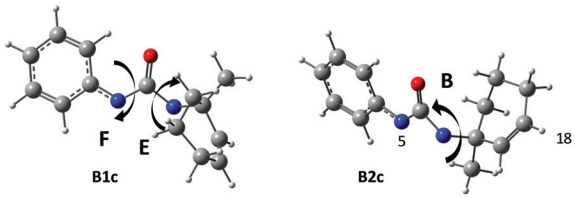

Fig. 6 Structure of the biradicalar intermediate **B1c** calculated at the DFT(B3LYP)/3-21G* level. Rotational degrees of freedom are related to dihedrals E [OCN(3)C(20)] and F [OCN(5)C(6)] (see Fig. 1 for atom numbering). In the minimum of **B2c** rotation of dihedral B, essential for ring closure through the approach of C(18) to N(5), occurs far from the plane of the carbamide moiety, preventing formation of putative pyrimidinone.

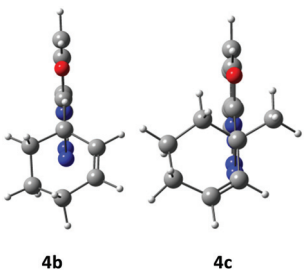

Fig. 7 Relative orientation of the cyclohex-2-enol and tetrazole rings (dihedral angle B) of the starting compounds, 4-allyl tetrazolones **4b** and **4c**, as a result of their different substituents H and CH_3 respectively.

Again, cleavage of the tetrazole ring with N_2 extrusion is assumed to lead to a biradicalar intermediate **B1c**, with two new rotational degrees of freedom, the dihedral angle E and the dihedral angle F (Fig. 6).

Three minima were found for anticlockwise rotation of dihedral E: the *cis* orientation, −60° and −90°. Interestingly in this structure, for the clockwise rotation of dihedral E, no structures corresponding to minima were found. Analysis of the initial structures **4b** and **4c** reveals a clear difference in the relative orientation of the cyclohex-2-enol and tetrazole rings (dihedral angle B) imposed by the two different substituents (Fig. 7). As mentioned above, the methylated tetrazolone **4c** exhibits three minima for the rotation of the CNC(20)C(21) (dihedral angle B), the *trans* and *gauche* orientations, the *gauche* (+61.4°) being the most stable conformer. This *gauche* conformation of the dihedral angle B prevents clockwise rotation around dihedral E in the intermediate **B1c**, due to steric hindrance caused by the methyl, justifying the observed product selectivity when the outcome of photolysis of compounds **4b** and **4c** is compared.

In both minima corresponding to dihedral E orientations of −60° and −90° (**B2c**, Fig. 6), rotation of dihedral B, essential for ring closure through the approach of C(18) to N(5), occurs far from the plane of the carbamide moiety. Thus, rotation of dihedral B is prevented due to steric hindrance and to increased difficulties in the ring closure process imposed by the geometry of **B2c**.

For the alternative route involving rotation of dihedral F in **B1c**, two minima were found, corresponding to the *cis* and *trans* orientations (**B2c′**; Fig. 8). Ring closure requires the approach of C(7) to N(3), providing the expected structure of benzimidazolone (**11**), in an exothermic process (Fig. 5 and 8).

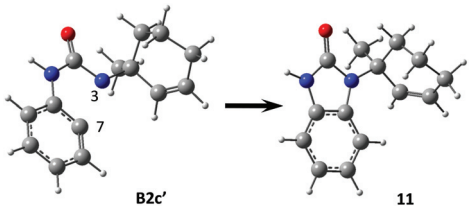

Fig. 8 Minimum energy structure obtained for biradicalar intermediate **B2c′**, found from the rotation of dihedral F, corresponding to the *trans* orientation. Minimum energy structure obtained for the expected structure of benzimidazolone **11**, obtained from **B2c′** by ring closure, through the approach of C(7) to N(3).

The experimental data are in agreement with results from theoretical calculations, showing a selective preference for the route leading to formation of benzimidazolone.

2.5. Investigation of the nature of the intermediate; flash photolysis experiments

Based on results of our preliminary investigation of the photochemistry of selected allyl tetrazolones (**4**; Scheme 1) we proposed a mechanism of photolysis involving initial photoextrusion of nitrogen with formation of a triplet biradical. This proposal was based on the observed photosensitizing effect of oxygen and also on the observation that an increase in solvent viscosity led to a decrease in quantum yields.[11] It was thus proposed from this evidence that photoexcitation of 1-allyl-4-phenyl-1,4-dihydro-5*H*-tetrazol-5-ones **4** would lead to formation of a caged triplet biradical that after T–S conversion would cyclize to the product.[11] Quast and co-workers had already postulated on the involvement of a transient biradical in formation of benzimidazolones from aryl-tetrazolones and tetrazole-thiones.[22] However, no flash photolysis or spin trap experiments were ever conducted to confirm the nature of the transient intermediate species involved.

In recent years, we undertook a mechanistic examination of the photodecomposition of 5-allyloxytetrazoles.[14] For this class, results from laser flash photolysis experiments revealed involvement of an excited triplet state and implicated the intermediacy of a triplet biradical in photolysis of allyloxy tetrazoles. More recently, Rayat and collaborators investigated the mechanism of photolysis of tetrazolethiones.[8] Based on the absence of an appreciable effect of the presence of triplet sensitizers (benzophenone, acetophenone and acetone) and triplet quenchers (biphenyl and oxygen) on the nature and quantities of photodecomposition products obtained from tetrazolethiones, the authors concluded against the involvement of a triplet excited state and (probably) triplet biradicals in the photolysis of tetrazolethiones.[8]

In order to gather further information on the nature of the intermediate involved in photolysis of 1-allyl-4-phenyl-1,4-dihydro-5*H*-tetrazol-5-ones we undertook laser flash photolysis experiments for compounds **4a–c**. A direct observation of the possible transient formed upon excitation at 266 nm was undertaken and its kinetics was followed in the presence and absence

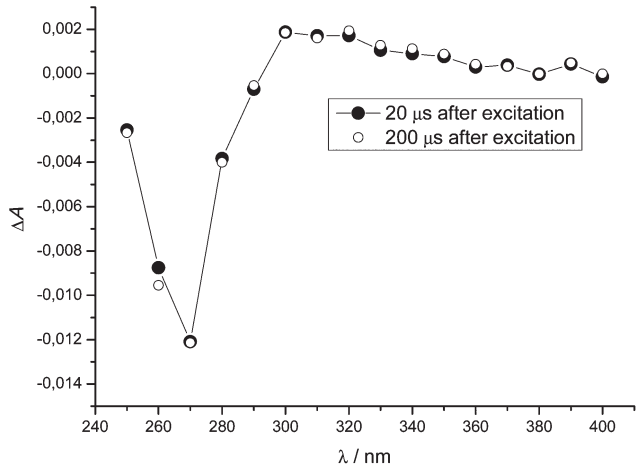

Fig. 9 Transient absorption for tetrazolone **4b**, following excitation at 266 nm. Circles: 20 μs after excitation; open circles: 200 μs after excitation.

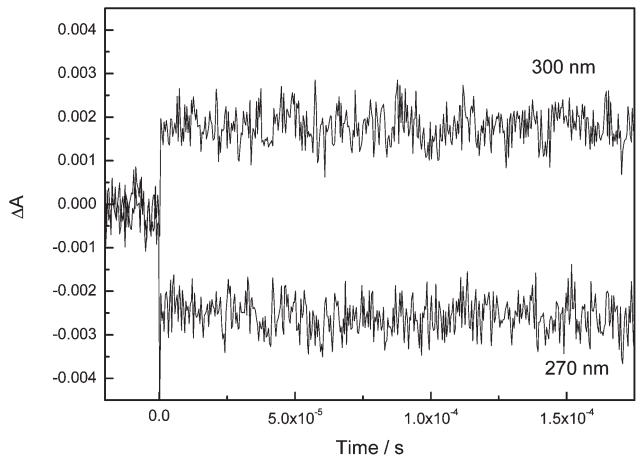

Fig. 10 Transient decay at 270 nm (depletion) and 300 nm observed in the presence of oxygen for tetrazolone **4c**.

of oxygen and with addition of the radical trap *N-tert*-butyl-α-phenylnitrone.[37,38] A biradical with a relatively long lifetime should be very sensitive to quenching by this agent[39] and such a study should provide further information on the spin nature of the intermediate involved in photodecomposition of 1-allyl-4-aryltetrazolones.

Fig. 9 shows the typical transient absorption spectra obtained for tetrazolone **4b**. A depletion band with a maximum at 270 nm is observed, followed by a band with a maximum at 300 nm that spreads until 360 nm. This figure shows that the transient absorption intensity does not change appreciably over a long period of time, as the transient spectra taken 20 and 200 μs after the laser pulse excitation completely overlap. The same happens on both observed bands, indicating the observation of a unique transient over the spectrum.

The decays observed for tetrazolone **4c** at the two transient absorption maxima (270 nm and 300 nm, Fig. 10) confirm the long lifetime of the transients. The same long-lived species is observed either in the presence or in the absence of oxygen. We did not observe any growth component on the kinetic traces taken, which indicates that the transient observed is formed within the 8 ns excitation laser pulse. In order to further investigate on the nature of the 300–360 nm absorbing transient, gathering evidence for either a neutral triplet state or radical species, the effect of *N-tert*-butyl-α-phenylnitrone on the transient species lifetime was also examined. Because competitive absorption of phenylnitrone did not allow us to collect the full range spectra we concentrated on the transient decay at 340 nm. Results have shown that the presence of phenylnitrone (concentration up to 1×10^{-4} M) does not change the observed decay at 340 nm, indicating that the transient observed may not be a triplet biradical. Similar behavior was observed for the three studied compounds (**4a–c)**.

Thus, our present results did not confirm the involvement of triplet states in photolysis of 1-allyl-4-aryltetrazolones. This observation is in keeping with results obtained for the photolysis of tetrazolethiones where participation of triplet states was also discarded.[8] However the evidence gathered is not sufficient to discard a triplet pathway. The DFT calculations assumed a biradical intermediate, and theoretical data comply with the nature of products obtained. Thus, the nature of the long-lived transient intermediate observed by flash photolysis remains to be clarified.

3. Conclusions

The photochemistry of tetrazolones derived from the carbocyclic allylic alcohols cyclohex-2-enol and 3-methylcyclohex-2-enol and from the natural terpene alcohol nerol was investigated in solution with the aim of assessing the effect of solvent and of structural constraints imposed by bulky allylic moieties on photoproduct selectivity and stability. Photolysis of tetrazolones derived from nerol and cyclohex-2-enol afforded the corresponding pyrimidinones as major products through a pathway that appears to be similar to that proposed for other 1-allyl-4-phenyl-1,4-dihydro-5*H*-tetrazol-5-ones derived from acyclic and unhindered allylic alcohols previously investigated by us but photolysis of the tetrazolone derived from the bulkier 3-methylcyclohex-2-enol **4c** leads to formation of a benzimidazolone, indicating that, in this case, cyclization of the transient intermediate species formed upon extrusion of N_2 involves the phenyl substituent and not the allylic moiety. Interpretation of the experimental results and of mechanistic pathways proposed was assisted by theoretical calculations (DFT(B3LYP)/3-21G*). This unexpected cyclization pathway is ascribed to steric constraints imposed by the methyl group attached to the allylic carbon in **4c**, which hinders the cyclization pathway involving the transient intermediate formed from **4c** and the allylic system, that would lead to formation of the expected pyrimidinone. Laser flash photolysis experiments were conducted with the aim of clarifying the nature of the intermediate involved in the primary photocleavage process. A unique long-lived transient was observed but its nature remains elusive.

4. Experimental section

4.1. Equipment and experimental conditions

All chemicals were used as purchased from Aldrich. Solvents for extraction and chromatography were of technical grade. When

required, solvents were freshly distilled from appropriate drying agents before use. Analytical TLC was performed with silica gel 60 F_{254} plates from Merck. Melting points were recorded on a Stuart Scientific SMP3 melting point apparatus and are uncorrected. UV absorption spectra were recorded on a Varian CARY 50 Bio UV-visible spectrophotometer, using 1 × 1 cm quartz cells. Mass spectra were obtained on a VG 7070E mass spectrometer by electron ionization (EI) or chemical ionization (CI, NH_3) at 70 eV. ^{1}H-NMR (400 MHz) spectra were obtained on a Bruker AM-400 spectrometer using TMS as the internal reference (δ = 0.0 ppm). Elemental analyses were performed on an EA1108-Elemental Analyzer (Carlo Erba Instruments). Infrared spectra were obtained on a Bruker FTIR-TENSOR 27 spectrometer. GC-MS analyses were carried out on a 6890-N Network GC System gas chromatograph with a 5973 inert Mass Selective Detector (EI 70 eV) from Agilent Technologies, using a DB-35MS capillary column with 30 m length and 0.25 mm ID (J & W Scientific, Agilent). The initial temperature of 50 °C was maintained during 3 min and then a heating rate of 10 °C min^{-1} was applied, until a final temperature of 250 °C was reached.

Photolysis studies were carried out in analytical grade acetonitrile, cyclohexane and methanol using 1 × 1 cm quartz cells at a distance of 10 to 40 cm from the lamp. A 16 W low-pressure Hg lamp (254 nm) was used as a source of UV radiation. Generally, 10^{-4} M starting solutions were used.

4.2. Computational details

Quantum chemical calculations were performed using the Gaussian 03 program package[40] at the DFT level of theory with the 3-21G* basis set and the three-parameter density functional, abbreviated as B3LYP, which includes Becke's gradient exchange correction[41] and the Lee, Yang, Parr correlation functional.[42] No symmetry restrictions were imposed on the initial structures.

4.3. Flash photolysis

Flash photolysis experiments were carried out on an Applied Photophysics LKS.60 laser-flash-photolysis spectrometer, with a Spectra-Physics Quanta-Ray GCR-130 Nd:YAG laser (fourth harmonic, 266 nm) for excitation and a Tektronix TDS3052B oscilloscope for transient decay capture. Sample solutions in acetonitrile were pumped through a quartz cell at a 0.9 mL min^{-1} flow rate using an SSI chromatographic pump.

4.4. Synthesis of 5-allyloxytetrazoles and 4-allyltetrazol-4-ones

4.4.1. (*E*)-5-(3,7-Dimethylocta-2,6-dienyloxy)-1-phenyl-1*H*-tetrazole (3a). (*E*)-3,7-Dimethylocta-2,6-dien-1-ol (nerol; 2.15 g; 13.9 mmol) in dry THF (20 mL) was added to a slurry of sodium hydride (60% in mineral oil; 0.60 g; 14.6 mmol) in dry THF (20 mL). When effervescence (hydrogen) had ceased (30 min) 5-chloro-1-phenyl-1*H*-tetrazole (2.5 g; 13.9 mmol), in dry THF (20 mL), was added, and the reaction was stirred at ≈10 °C for 12 h. Work-up followed by crystallization of the solid residue from ethanol gave the required product as white crystals (1.0 g; 24% yield), mp 43–45 °C. IR ν_{max}: 2967, 2912, 2858, 1592, 1570, 1506, 1460, 1443, 939; ^{1}H NMR (400 MHz, CD_3OD): δ 1.56 (3H, s, CH_3), 1.60 (3H, s, CH_3), 1.81 (3H, s, CH_3), 2.09–214 (2H, q, CH_2), 2.21–2.25 (2H, t, CH_2), 5.09, 5.10 (3H, d,=CH–, CH_2), 5.58–5.61 (1H, t,=CH–), 7.48–7.52 (1H, m, ArH), 7.55–7.58 (2H, t, ArH), 7.70,7.72 (2H, d, ArH).

4.4.2. 1-(3,7-Dimethylocta-1,6-dien-3-yl)-4-phenyl-1*H*-tetrazol-5(4*H*)-one (4a). A neat sample of (*E*)-5-(3,7-dimethylocta-2,6-dienyloxy)-1-phenyl-1*H*-tetrazole (0.8 g; 2.7 mmol) was heated at 40 °C for 1 h to give 1-(cyclohex-2-enyl)-4-phenyl-1*H*-tetrazol-5(4*H*)-one as a yellow oil (quantitative yield). IR ν_{max}: 1725, 1598, 1560, 1502, 1376, 757 cm^{-1}; ^{1}H NMR (400 MHz, $CDCl_3$): δ 1.54 (3H, s, CH_3), 1.57 (3H, s, CH_3), 1.77 (3H, s, CH_3), 1.98–2.37 (4H, m, –CH_2CH_2–), 5.01–5.07 (1H, t,=CH–), 5.16–5.25 (2H, m,=CH_2), 623–6.30 (1H, m,=CH–), 7.36–7.40 (1H, t, ArH), 7.48–7.52 (2H, t, ArH), 7.85, 7.87 (2H, d, ArH); ^{13}C NMR (100 MHz, CD_3OD): δ_C 16.37, 21.69, 22.19, 24.54, 36.97, 64.95, 113.63, 119.38, 122.75, 127.53, 129.03, 131.75, 134.55, 139.51, 148.76; MS (EI), *m*/*z* 299 $[M + H]^+$; Anal. Calcd for $C_{17}H_{22}N_4O$: C, 68.43; H, 7.43; N, 18.78%. Found: C, 68.22; H, 7.75; N, 18.30%.

4.4.3. 5-(Cyclohex-2-enyloxy)-1-phenyl-1*H*-tetrazole (3b). Cyclohex-2-enol (1.36 g; 13.9 mmol) in dry THF (30 mL) was added to a slurry of sodium hydride (55% in mineral oil; 0.65 g; 14.9 mmol) in dry THF (5 mL). When effervescence of hydrogen had ceased (30 min), 5-chloro-1-phenyl-1*H*-tetrazole (2.5 g; 13.9 mmol) in dry THF (20 mL) was added and the final mixture was stirred at room temperature for about 3 h. Work-up and crystallization of the crude from ethanol gave the 5-(cyclohex-2-enyloxy)-1-phenyl-1*H*-tetrazole as white crystals (2.1 g; 61% yield), mp 60–62 °C. IR ν_{max}: 2927, 1591, 1549, 1504, 1457, 910 cm^{-1}; ^{1}H NMR (400 MHz, CD_3OD): δ 1.66–1.83 (2H, m, –CH_2–), 2.04–2.18 (4H, m, –CH_2–), 5.47–5.48 (1H, m, CH–O–), 5.98, 6.00 (1H, d, –CH=), 6.09–6.13 (1H, m,=CH–), 7.47–7.51 (1H, t, ArH), 7.54–7.58 (2H, t, ArH), 7.70–7.72 (2H, d, ArH); ^{13}C NMR (100 MHz, CD_3OD): δ_C 18.06, 24.64, 27.87, 78.52, 121.85, 123.44, 128.98, 129.44, 133.47, 134.91, 159.85; MS (EI), *m*/*z* 242 $[M]^+$.

4.4.4. 4-(Cyclohex-2-enyl)-1-phenyl-1*H*-tetrazol-5(4*H*)-one (4b). A neat sample of 5-(cyclohex-2-enyloxy)-1-phenyl-1*H*-tetrazole (1.0 g; 4.1 mmol) was heated at 40 °C for 2 h to give 1-(cyclohex-2-enyl)-4-phenyl-1*H*-tetrazol-5(4*H*)-one as a yellow oil (quantitative yield). IR ν_{max}: 2927, 1724, 1595, 1552, 1504, 1459, 904 cm^{-1}; ^{1}H NMR (400 MHz, CD_3OD): δ 1.71–2.23 (6H, m, –CH_2–), 4.88–4.91 (1H, m, CH–N), 5.71–5.74 (1H, d, –CH=), 6.08–6.10 (1H, m=CH–), 7.39–7.42 (1H, t, ArH), 7.50–7.54 (2H, t, ArH), 7.87–7.89 (2H, d, ArH); ^{13}C NMR (100 MHz, $CDCl_3$): δ_C 20.14, 24.78, 28.70, 52.03, 77.14, 77.45, 77.77, 119.71, 124.31, 127.98, 129.73, 133.45, 135.19; MS (EI), *m*/*z* 243 $[M + H]^+$.

4.4.5. 4-(3-Methylcyclohex-2-enyl)-1-phenyl-1*H*-tetrazol-5(4*H*)-one (4c). 3-Methyl-cyclohex-2-enol (0.62 g; 5.54 mmol) in dry THF (30 mL) was added to a slurry of sodium hydride (55% in mineral oil; 0.32 g; 7.4 mmol) in dry THF (5 mL). When effervescence (hydrogen) had ceased (20 min) 5-chloro-1-phenyl-1*H*-tetrazole (1.0 g; 5.54 mmol) in dry THF (10 mL) was added, and the mixture was stirred at ≈10 °C for 4 h. 4-(3-

Methylcyclohex-2-enyl)-1-phenyl-1*H*-tetrazol-5(4*H*)-one was obtained as a light yellow oil (1.1 g; 71% yield), indicating that the synthesised ether readily isomerises to the corresponding tetrazolone **4c**. IR ν_{max}: 2927, 1721, 1596, 1504, 1460, 1367, 1095, 904 cm^{-1}; ^{1}H NMR (400 MHz, CD_3OD): δ 1.69 (3H, s, CH_3), 1.79–1.86 (4H, m, $–CH_2CH_2–$), 2.09–2.11 (2H, m, CH_2), 5.97–6.03 (2H, m, CH═CH), 7.38–7.42 (1H, t, ArH), 7.50–7.54 (2H, t, ArH), 7.85–7.87 (2H, d, ArH); ^{13}C NMR (100 MHz, CD_3OD): δ_C 18.34, 24.21, 25.29, 32.78, 60.16, 119.63, 127.59, 128.15, 129.05, 130.50, 134.59, 148.71; MS (EI), *m*/*z* 257 $[M + H]^+$.

4.5. Preparation of compounds 10a,b and 11 (preparative scale irradiations)

4.5.1. 4-Methyl-4-(4-methylpent-3-enyl)-1-phenyl-3,4-dihydropyrimidin-2(1*H*)-one (10a). 1-(3,7-Dimethylocta-1,6-dien-3-yl)-4-phenyl-1*H*-tetrazol-5(4*H*)-one **4a** (0.05 g; 0.17 mmol) in methanol (75 ml) was irradiated at λ = 254 nm with continuous stirring, with the cell at a distance of 10 cm from a 16 W low pressure Hg lamp until no starting material was detected by GC-MS analysis (40 min). The final solution was removed, the solvent was evaporated and the major photoproduct was isolated by column chromatography on silica gel, using a mixture of hexane and ethyl acetate as an eluent. The isolated compound was collected as a colorless oil (0.038 g; 83% yield) and identified as 4-methyl-4-(4-methylpent-3-enyl)-1-phenyl-3,4-dihydropyrimidin-2(1*H*)-one, **10a**. IR ν_{max}: 2973, 2870, 1669, 1592, 1262 cm^{-1}; ^{1}H-NMR (400 MHz, CD_3OD): δ 1.26 (3H, s); 1.41 (3H, s); 1.57 (3H, s); 1.75–1.86 (2H, m); 2.01–2.39 (2H, m); 4.06–4.12 (1H, m); 5.06 (1H, d, J = 10.5 Hz); 5.23 (1H, d, J = 4.9 Hz); 6.88–6.92 (3H, m); 7.15 (2H, t, J = 7.8 Hz); ^{13}C NMR (100 MHz, CD_3OD): δ_C 23.40, 23.77, 24.78, 25.95, 43.71, 51.21, 63.72, 71.06, 112.36, 123.58, 127.96, 128.51, 142.79, 148.06, 151.54; MS (EI), *m*/*z* 270 $[M]^+$.

Similarly, the other compounds were prepared and isolated.

4.5.2. 1-Phenyl-3a,4,5,6-tetrahydro-1*H*-benzoimidazol-2(3*H*)-one (10b). 4-(Cyclohex-2-enyl)-1-phenyl-1*H*-tetrazol-5(4*H*)-one **4b** (0.05 g; 0.20 mmol), irradiated for 15 min, gave a brown solid (0.025 g; 56% yield). IR ν_{max}: 3327, 3063, 2937, 2867, 1690, 1548 cm^{-1}; ^{1}H-NMR (400 MHz, CD_3OD): δ 0.90–0.95 (1H, m); 1.27–1.32 (5H, m); 3.34–3.38 (1H, t); 5.09(1H, m); 6.99–7.02 (1H, t, ArH); 7.25–7.29 (2H, t, ArH); 7.40–7.42 (2H, d, ArH); MS (EI), *m*/*z* 214 $[M]^+$.

4.5.3. 3-(1-Methylcyclohex-2-enyl)-benzoimidazol-2(1*H*)-one (11). 4-(3-Methylcyclohex-2-enyl)-1-phenyl-1*H*-tetrazol-5(4*H*)-one **4c** (0.05 g; 0.19 mmol) was irradiated for 20 min. Isolation afforded a yellow powder (0.034 g; 76% yield). IR ν_{max}: 3124, 3006, 2921, 1687, 1475, 1360 cm^{-1}; ^{1}H-NMR (400 MHz, CD_3OD): δ 1.52–1.75 (4H, m); 1.83 (3H, s); 2.11–2.15 (2H, m); 6.02 (1H, dt, J = 10.1 Hz, J = 3.5 Hz); 6.09 (1H, d, J = 10.1 Hz); 6.91–7.01 (3H, m); 7.60 (1H, d, J = 8.0 Hz); ^{13}C NMR (100 MHz, CD_3OD): δ_C 18.78, 24.58, 26.55, 33.18, 58.31, 108.56, 112.08, 120.16, 120.68, 128.55, 129.12, 130.92, 132.72, 155.47; MS (EI), *m*/*z* 228 $[M]^+$.

Acknowledgements

The authors acknowledge Fundação para a Ciência e Tecnologia (FCT) and FEDER [Projects PTDC/QUI/67674/2006 and PTDC/QUI/71203/2006] for financial support.

References

1 S. C. S. Bugalho, E. M. S. Macoas, M. L. S. Cristiano and R. Fausto, Low temperature matrix-isolation and solid state vibrational spectra of tetrazole, *Phys. Chem. Chem. Phys.*, 2001, **3**, 3541–3547.
2 Y. Tamura, F. Watanabe, T. Nakatani, K. Yasui, M. Fuji, T. Komurasaki, H. Tsuzuki, R. Maekawa, T. Yoshioka, K. Kawada, K. Sugita and M. Ohtani, Highly selective and orally active inhibitors of type IV collagenase (MMP-9 and MMP-2): N-sulfonylamino acid derivatives, *J. Med. Chem.*, 1998, **41**, 640–649.
3 G. Maier, J. Eckwert, A. Bothur, H. P. Reisenauer and C. Schmidt, Photochemical fragmentation of unsubstituted tetrazole, 1,2,3-triazole, and 1,2,4-triazole: first matrix-spectroscopic identification of nitrilimine HCNNH, *Liebigs Ann.*, 1996, 1041–1053.
4 A. Gomez-Zavaglia, I. D. Reva, L. Frija, M. L. Cristiano and R. Fausto, Molecular structure, vibrational spectra and photochemistry of 2-methyl-2*H*-tetrazol-5-amine in solid argon, *J. Phys. Chem. A*, 2005, **109**, 7967–7976.
5 A. Ismael, M. L. S. Cristiano, R. Fausto and A. Gomez-Zavaglia, Tautomer selective photochemistry in 1-(tetrazol-5-yl)ethanol, *J. Phys. Chem. A*, 2010, **114**, 13076–13085.
6 A. Gomez-Zavaglia, I. D. Reva, L. Frija, M. L. Cristiano and R. Fausto, Photochemistry of 1-phenyl-tetrazolone isolated in solid argon, *J. Photochem. Photobiol., A*, 2006, **179**, 243–255.
7 A. Gomezzavaglia, I. Reva, L. Frija, M. Cristiano and R. Fausto, Molecular structure, vibrational spectra and photochemistry of 5-mercapto-1-methyltetrazole, *J. Mol. Struct.*, 2006, **786**, 182–192.
8 O. E. Alawode, C. Robinson and S. Rayat, Clean photodecomposition of 1-methyl-4-phenyl-1*H*-tetrazole-5(4*H*)-thiones to carbodiimides proceeds *via* a biradical, *J. Org. Chem.*, 2011, **76**, 216–222.
9 A. Gómez-Zavaglia, I. D. Reva, L. Frija, M. L. S. Cristiano and R. Fausto, Infrared spectrum and UV-induced photochemistry of matrix-isolated 5-methoxy-1-phenyl-1*H*-tetrazole, *J. Photochem. Photobiol., A*, 2006, **180**, 175–183.
10 L. M. T. Frija, I. V. Khmelinskii and M. L. S. Cristiano, Novel efficient synthesis of 3,4-dihydro-6-substituted-3-phenylpyrimidin-2(1*H*)-ones, *Tetrahedron Lett.*, 2005, **46**, 6757–6760.
11 L. M. T. Frija, I. V. Khmelinskii and M. L. S. Cristiano, Mechanistic investigations into the photochemistry of 4-allyl-tetrazolones in solution: a new approach to the synthesis of 3,4-dihydro-pyrimidinones, *J. Org. Chem.*, 2006, **71**, 3583–3591.
12 L. M. T. Frija, I. D. Reva, A. Gomez-Zavaglia, M. L. S. Cristiano and R. Fausto, UV-induced photochemistry of matrix-isolated 1-phenyl-4-allyl-tetrazolone, *Photochem. Photobiol. Sci.*, 2007, **6**, 1170–1176.
13 L. M. T. Frija, I. D. Reva, a Gómez-Zavaglia, M. L. S. Cristiano and R. Fausto, Photochemistry and vibrational spectra of matrix-isolated 5-ethoxy-1-phenyl-1*H*-tetrazole, *J. Phys. Chem., A*, 2007, **111**, 2879–2888.
14 L. M. T. Frija, I. V. Khmelinskii, C. Serpa, I. D. Reva, R. Fausto and M. L. S. Cristiano, Photochemistry of 5-allyloxy-tetrazoles: steady-state and laser flash photolysis study, *Org. Biomol. Chem.*, 2008, **6**, 1046–1055.
15 I. R. Dunkin, C. J. Shields and H. Quast, The photochemistry of 1,4-dihydro-5*H*-tetrazole derivatives isolated in low-temperature matrices, *Tetrahedron*, 1989, **45**, 259–268.
16 H. Quast and L. Bieber, Phtotochemical formation of methylenecyclopropane analogs. 1. Aziridinimines, diaziridinimines, diaziridinones, and carbodiimides by photolysis of 2-tetrazolines, *Angew. Chem., Int. Ed. Engl.*, 1975, **14**, 428–429.
17 I. R. Dunkin, The infrared-spectrum, light-induced infrared linear dichromism and conformatioanl-analysis of phenyl azide in solid nitrogen at 12-K, *Spectrochim. Acta, Part A*, 1986, **42**, 649–655.
18 A. Gómez-Zavaglia, I. Reva, L. M. Frija, M. L. Cristiano and R. Fausto, *Photochemistry of Tetrazole Derivatives in Cryogenic Rare Gas Matrices, Photochemistry Research Progress*, Nova Publishers, New York, NY, USA, 2008, pp. 295–234.

19 A. Gómez-Zavaglia, I. D. Reva, L. M. T. Frija, M. L. S. Cristiano and R. Fausto, Photochemistry of tetrazole derivatives in cryogenic rare gas matrices, *Chem. Phys. Res. J.*, 2009, **1**, 221–250.

20 H. Quast and L. Bieber, Photochemical-synthesis of methylencyclopropane analogs. 5. Synthesis and photolysis of 1,4-dialkyl-1,4-dihydro-5*H*-tetrazol-5-ones and 1,4-dialkyl-1,4-dihydro-5*H*-tetrazol-5-thiones: a novel approach to diaziridinones and carbodiimides, *Chem. Ber. Recl.*, 1981, **114**, 3253–3272.

21 H. Quast, A. Fuss and U. Nahr, Photochemical formation of methylene cyclopropane analogs. 11. Photochemical elimination of molecular nitrogen from phenyl-substituted 1,4-dihydro-5-imino-5*H*-tetrazoles-products of phenyl substituted tris(imino)methane diradicals, *Chem. Ber. Recl.*, 1985, **118**, 2164–2185.

22 H. Quast and U. Nahr, Photoextrusion of nitrogen from 1,4-dihydro-1-phenyl-5*H*-tetrazol-5-ones and 5-thiones-benzimidazolones and carbodiimides, *Chem. Ber. Recl.*, 1985, **118**, 526–540.

23 H. Quast, Some recent advances in the synthesis of 3-membered ring heterocycles, *Heterocycles*, 1980, **14**, 1677–1702.

24 J. A. Hyatt and J. S. Swenton, Photochemistry in tetrazole-azidoazomethine system – facile synthesis of 9*H*-pyrimido 4,5-B indoles, *J. Org. Chem.*, 1972, **37**, 3216–3220.

25 H. Quast and U. Nahr, Phtochemical formation of methylenecyclopropane analogs. 8. Photoextrusion of nitrogen from 1-alkenyl-4-alkyl-1,4-dihydro-5*H*-tetrazol-5-ones and 1-alkenyl-4-alkenyl-4-alkyl-1,4-dihydro-5*H*-tetrazol-5-thiones-diaziridinon, *Chem. Ber. Recl.*, 1983, **116**, 3427–3437.

26 H. Quast, A. Fuss and W. Nudling, Photochemical formation of heteromethylenecyclopropanes, 28 - photoextrusion of molecular nitrogen from annulated 5-alkylidene-4,5-dihydro-1*H*-tetrazoles: annulated iminoaziridines and the first triplet diazatrimethylenemethane, *Eur. J. Org. Chem.*, 1998, 317–327.

27 H. Quast and L. W. Bieber, Iminodiaziridines by regio- and stereoselective cyclization of diastereomeric singlet triazatrimethylenemethane diradicals generated through photolysis of 5-imino-4,5-dihydro-1*H*-tetrazoles, *J. Org. Chem.*, 2008, **73**, 3738–3744.

28 L. M. T. Frija, A. Ismael and M. L. S. Cristiano, Photochemical transformations of tetrazole derivatives: applications in organic synthesis, *Molecules*, 2010, **15**, 3757–3774.

29 S. C. Bugalho, L. Lapinski, M. L. S. Cristiano, L. M. Frija and R. Fausto, Vibrational spectra and structure of 1-phenyltetrazole and 5-chloro-1-phenyltetrazole, *Vib. Spectrosc.*, 2002, **30**, 213–225.

30 M. L. S. Cristiano and R. A. W. Johnstone, A kinetic investigation of the thermal rearrangement of allyloxytetrazoles to N-allyltetrazolones, *J. Chem. Soc., Perkin Trans. 2*, 1997, 489–494.

31 M. L. S. Cristiano and R. A. W. Johnstone, Intramolecularity of the thermal rearrangement of allyloxytetrazoles to n-allyltetrazolones, *J. Chem. Res.-S*, 1997, 164–165.

32 N. C. P. Araujo, P. M. M. Barroca, J. F. Bickley, A. F. Brigas, M. L. S. Cristiano, R. A. W. Johnstone, R. M. S. Loureiro and P. C. A. Pena, Structural effects on sigmatropic shifts in heteroaromatic allyl ethers, *J. Chem. Soc., Perkin Trans. 1*, 2002, 1213–1219.

33 L. M. T. Frija, I. Reva, A. Ismael, D. V. Coelho, R. Fausto and M. L. S. Cristiano, Sigmatropic rearrangements in 5-allyloxytetrazoles, *Org. Biomol. Chem.*, 2011, **9**, 6040–6054.

34 S. Wang, L. Wu, L. Zhang and C. Tung, Supramolecular assemblies based on 2-ureido-4[1*H*]-pyrimidinone building block, *Chin. Sci. Bull.*, 2006, **51**, 129–138.

35 R. F. Klima and A. D. Gudmundsdóttir, Intermolecular triplet-sensitized photolysis of alkyl azides, *J. Photochem. Photobiol., A*, 2004, **162**, 239–247.

36 M. Cignitti, M. C. Ramusino and L. Rufini, UV spectroscopic study and conformational analysis of domperidone, *J. Mol. Struct.*, 1995, **350**, 43–47.

37 E. G. Janzen, Spin trapping, *Acc. Chem. Res.*, 1971, **4**, 31–40.

38 Y.-T. Park, N. W. Song, Y.-H. Kim, C.-G. Hwang, S. K. Kim and D. Kim, Flash photolysis observation of aryl, 2,3-dihydrocyclohexadienyl, and halogen anion radicals in aqueous solution: photohomolytic radical cyclization of aryl halide 1, *J. Am. Chem. Soc.*, 1996, **118**, 11399–11405.

39 B. Halliwell and J. M. C. Gutteridge, *Free Radicals in Biology and Medicine*, Oxford University Press, London, 3rd edn., 1998.

40 M. J. Frisch, G. W. Trucks, H. B. Schlegel, G. E. Scuseria, M. A. Robb, J. R. Cheeseman, J. A. Montgomery, T. Vreven Jr., K. N. Kudin, J. C. Burant, J. M. Millam, S. S. Iyengar, J. Tomasi, V. Barone, B. Mennucci, M. Cossi, G. Scalmani, N. Rega, G. A. Petersson, H. Nakatsuji, M. Hada, M. Ehara, K. Toyota, R. Fukuda, J. Hasegawa, M. Ishida, T. Nakajima, Y. Honda, O. Kitao and H. Nakai, *GAUSSIAN 03 (Revision C.02)*, Gaussian, Inc., Wallingford, CT, 2004.

41 A. D. Becke, Density-functional exchange-energy approximation with correct asymptotic-behavior, *Phys. Rev. A*, 1988, **38**, 3098–3100.

42 C. T. Lee, W. T. Yang and R. G. Parr, Development of the Colle-Salvetti correlation-energy formula into a functional of the electron-density, *Phys. Rev. B*, 1988, **37**, 785–789.